Proceedings World Geothermal Congress 2026
Calgary, Canada, June 8 – 11, 2026

Offshore Geothermal: The Size of the Prize

Rebecca Bolton*, Rob Crossley, Alex Jones and Mark Williams
Viridien
rebecca.bolton@viridiengroup.com

Keywords: Offshore geothermal energy, Heat-flow modelling, Renewable baseload power, Global resource assessment

INTRODUCTION

Offshore geothermal energy is emerging as a strategic and scalable opportunity for clean, continuous power generation. The white paper, Offshore Geothermal: A Green Energy Resource of Global Significance and Its Responsible Development (Bolton et al., 2024), drew global attention to the vast heat potential stored within the magmatically active seafloor and flooded continental rift systems. It framed offshore geothermal energy as a cornerstone of future baseload supply, highlighting opportunities for integration with hydrogen, freshwater, and ammonia production and outlining a responsible development pathway (Figure 1).

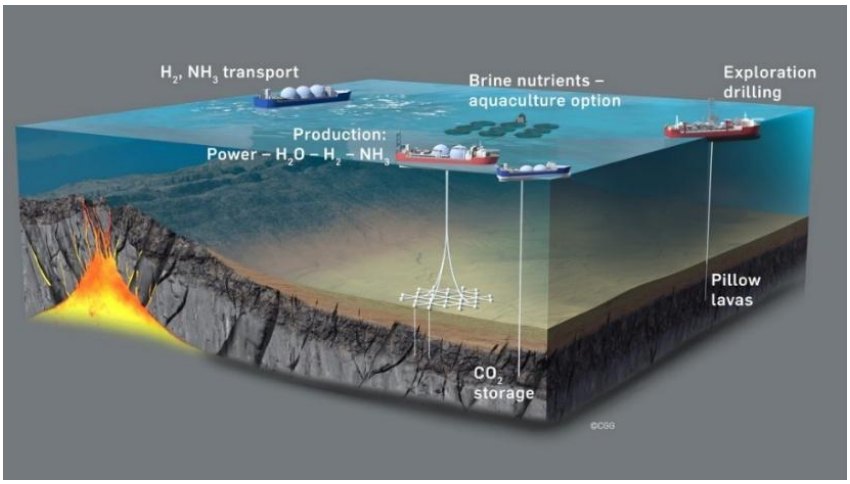


Figure 1. Conceptual schematic of an offshore geothermal energy system (Viridien, 2024). Heat extracted from young oceanic crust and underlying magmatic sources drives subsea power generation integrated with CO_2 storage and co-production of hydrogen, ammonia, and mineral-rich brines for onshore transport and utilisation.

Hydrothermal circulation in oceanic crust has been observed for decades at deep-sea vents and spreading ridges (Elderfield and Schultz, 1996), yet its potential as a recoverable energy resource has only recently come into focus. The underlying geophysical datasets; heat flow, crustal structure, and magnetic field measurements, have long existed, but advances in global data integration, subsurface modelling, and offshore engineering now make it possible to quantify this resource in physical and economic terms. Bolton et al. (2024) articulated this emerging opportunity in conceptual and strategic terms; the present study provides the quantitative foundation.

Building directly on that framework, the application of a physics-based, data-driven modelling approach is used to estimate the recoverable offshore geothermal resource at a global scale, the “size of the prize.” The analysis integrates basin-scale thermal modelling, geophysical parameters, and regional heat-flow data to identify where geological and operational conditions converge to make offshore geothermal power technically and economically viable.

1 MODELLING FRAMEWORK

1.1 Spatial and Physical Domain

The global offshore area was subdivided into a lattice of hexagonal grid cells using the H3 geospatial indexing framework (Uber Technologies, 2025). Each cell was modelled as a vertical column extending from the seafloor to the Curie isotherm (580 °C), allowing local geothermal gradients to be computed from regional geophysical

inputs. These inputs included seafloor temperature data from global ocean climatologies (Boyer et al., 2005), Curie depth estimates derived from magnetic anomaly inversions (Li et al., 2017), and crustal and sedimentary thicknesses from the CRUST1.0 model and NOAA compilations (Laske et al., 2013; Straume et al., 2019). To maintain engineering realism, areas deeper than 3 km of water or requiring wells beyond 3 km below the seafloor were excluded from the analysis (Jones et al., 2025).

For each grid cell, temperature as a function of depth was computed under two bounding thermal regimes. In the conductive scenario (Figure 2a), heat transfer was modelled as steady-state conduction through multiple layers with variable sediment and crustal thermal conductivities. In the conductive–convective scenario (Figure 2b), hydrothermal circulation was introduced above approximately 400 m below the seafloor, capped by the local boiling point at seafloor pressure and bounded below by the Curie isotherm. The crust was represented as a four-layer structure mantle, igneous crust, deep sediment, and an upper low-conductivity blanket, with continuity of heat flux maintained across all interfaces (Figure 2).

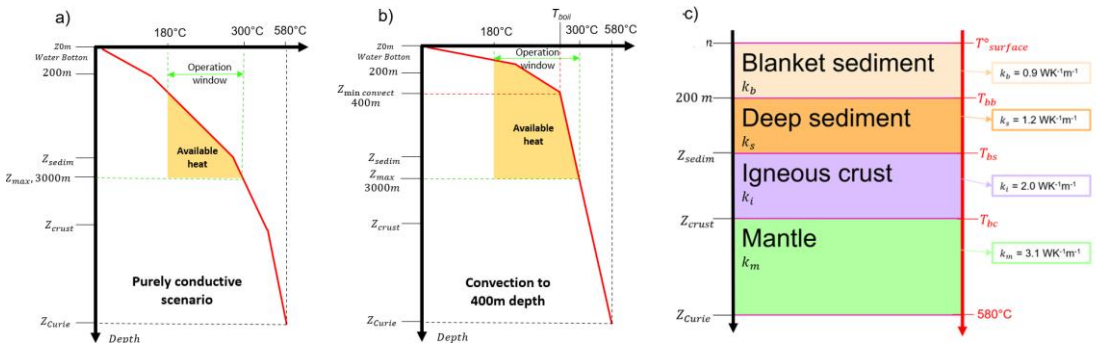


Figure 2. Conceptual heat-flow models illustrating (a) conductive, (b) conductive–convective, and (c) layered crustal configurations. *Reproduced from Jones et al. (2025).*

The global datasets described in Jones et al. (2025) provide both the boundary conditions and geometric framework of the model. The Curie depth, representing the 580 °C isotherm derived from magnetic anomaly inversions, defines the lower thermal boundary, while seafloor temperature from oceanographic climatologies defines the upper boundary. Between these limits, crustal and sediment thicknesses (from CRUST1.0 and NOAA compilations) determine the conductive path length and thermal resistance within each vertical column. Thinner crust promotes elevated heat flux, whereas thick, low-conductivity sedimentary successions act as insulating layers that suppress near-surface gradients.

The temperature profile within each column is computed using a one-dimensional steady-state conductive geotherm, expressed as formula 1.

$$T(z) = T_{seafloor} + \frac{T_{curie} - T_{seafloor}}{z_{curie}} z \tag{1}$$

Where $T(z)$ is the temperature at depth Z, $T_{seafloor}$ and T_{curie} are the temperatures at the upper and lower boundaries respectively, and z_{curie} is the depth to the Curie isotherm.

Together, these parameters form a consistent, data-driven representation of the subsurface, enabling calculation of temperature distributions, isotherm depths, and total heat flow for every grid cell across the global offshore domain (Figure 3).

1.2 Heat in Place

For each grid cell, the volumetric Heat in Place (HIP) was calculated from the temperature–depth profiles derived in Section 1.1. The HIP represents the total thermal energy stored within the rock–fluid system between a defined minimum and maximum temperature range and is given by equation (2).

$$Q_T = h * \frac{(T_{min} - T_{max})\left[\left((1-\phi) * C_r * \rho_r\right) + (\phi * C_w * \rho_w)\right]}{A} \tag{2}$$

Where A is the grid-cell area, h the thickness of the thermally active interval, ϕ the porosity, ρ_r and C_r the density and specific heat capacity of the rock matrix, and ρr and Cr those of the pore fluid. T_{min} and T_{max} represent the

upper and lower temperature limits, respectively. In this study, T_{max} = 300 °C and T_{min} = 180 °C were used to define the practical extractable temperature range, consistent with the operating envelope of high-enthalpy geothermal systems.

Representative rock and fluid properties were assigned from published averages for marine basalts and sediments (e.g., Clauser and Huenges, 1995; Vosteen and Schellschmidt, 2003), with fluid parameters corresponding to seawater salinity at in-situ pressure and temperature. The porosity term provides a weighted contribution from both the solid matrix and the interstitial fluid, capturing the total thermal storage capacity of the system.

The resulting Q_T values quantify the theoretical thermal energy stock within each cell in joules, independent of any engineering or economic constraints. These data form the basis for the estimation of recoverable power, where recovery efficiency and conversion factors are applied to determine the proportion of stored heat that can be realistically harnessed (Section 1.3).

1.3 Conversion to Recoverable power

The total heat in place for each cell was integrated and converted to electrical output following the approach of Jones et al. (2025) as shown in equation (3).

$$MWe = \frac{F_r * c_e}{F_l * t_r} * Q_T \tag{3}$$

Where Q_T is the total thermal energy in place (J m^{-2}) calculated in 1.2, F_r the recovery factor representing the proportion of reservoir heat that can be technically extracted, c_e is the thermal-to-electric conversion efficiency, F_l is the load factor accounting for plant availability, and t_r is the replenishment time reflecting the thermal recharge interval.

Parameters used were chosen based on operational benchmarks from modern binary-cycle geothermal plants: a recovery factor of 20 %, a conversion efficiency of 10 %, and a load factor of 95 %, assuming a one-year replenishment period. These values were applied uniformly across the global grid to derive recoverable power density (MWe km^{-2}). A representative production footprint of 16 km^2 was then used to estimate the generating capacity of a typical offshore geothermal installation.

2 RESULTS

Under purely conductive assumptions, global recoverable offshore geothermal power totals approximately 6 TWe. Mean recoverable power density is 0.07 MWe km^{-2}, with the 90th percentile approaching 3 MWe km^{-2}. Including convective heat transfer increases local power densities to 2–3 MWe km^{-2}, corresponding to plant-scale outputs of 100–120 MWe in favourable settings.

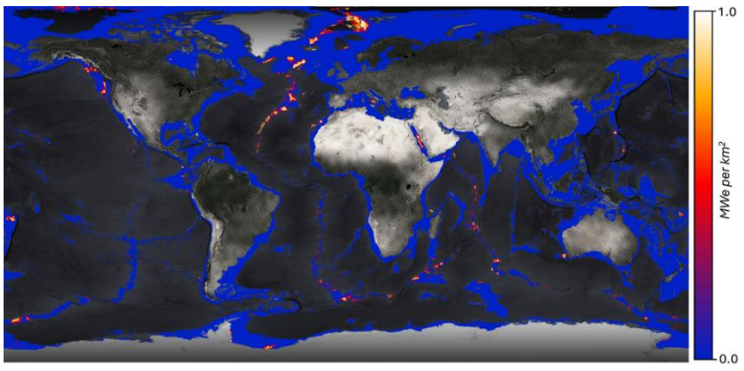


Figure 3. Global distribution of offshore geothermal resources, based on a quantitative physics based model. *Reproduced from Jones et al. (2025).* High-potential areas coincide with mid-ocean ridges, young oceanic crust, and actively rifting continental margins, where thin crust and elevated heat flow (> 400 mW m^{-2}) bring high temperatures within drilling reach. Notable examples include the Red Sea, East African Rift margins, the Icelandic Plateau, and the Arctic–North Atlantic region near Svalbard.

3 DISCUSSION: THE SCALE OF THE PRIZE

The modelled 6 TWe global resource represents roughly twice the world's current electricity generation capacity and more than 500 times today's installed geothermal power (IEA, 2025). Even utilisation of just 1 % of this theoretical potential could deliver tens of gigawatts of firm, low-carbon electricity. The quantitative outputs of this model provide a first-order screening tool to support early-stage comparison and prioritisation of offshore geothermal sites, aligning with the responsible-development framework outlined in Bolton et al. (2024) white paper. The global heat-flow analysis identifies the same first-order target domains emphasised by Viridien, mid-ocean ridges, rifted continental margins, and young oceanic crust, while constraining their potential output and areal extent. In doing so, the model bridges the gap between conceptual assessment and quantitative feasibility, confirming that the offshore resource base is sufficient to justify focused exploration and pilot-scale development.

The spatial variability revealed by the model also provides important context for the conceptual system illustrated in Figure 1, in which heat extraction supports not only subsea power generation but also integrated CO_2 storage and the co-production of hydrogen, ammonia, and mineral-rich brines. Because these cascading uses shape the underlying value proposition, future techno-economic assessments should reflect the likelihood that development pathways will differ from location to location, influenced by variations in thermal gradient, resource depth, infrastructure proximity, and market demand. As a result, offshore geothermal economics will be strongly site-specific, with distinct use cases and revenue architectures emerging across different geological settings. The model therefore offers not only a resource estimate but also a spatial framework for identifying where integrated offshore geothermal systems may achieve favourable techno-economic performance.

4 CHALLENGES, UNCERTAINTIES & FUTURE WORK

The model assumes steady-state thermal replenishment and does not simulate reservoir depletion. In reality, sustained production causes local cooling and pressure decline. Offshore systems remain untested, but the seawater-recharged Reykjanes field in southwest Iceland provides a useful analogue (Arnórsson, 1978; Friðleifsson et al., 2020). Despite transient pressure and temperature changes, no long-term heat-source decline has been observed, suggesting conductive replenishment can sustain output. Whether similar behaviour occurs in deeper, fully subsea settings remains uncertain due to limited monitoring data.

Model uncertainty arises from data resolution and simplifications. Curie-depth estimates from magnetic inversions are sensitive to crustal composition, and offshore heat-flow and borehole data remain sparse, limiting calibration. Consequently, results should be viewed as first-order spatial trends rather than precise local predictions.

Thermal and geological heterogeneity are also under-represented. Processes such as anisotropic conduction, fault-guided advection, and hydrothermal upflow could locally modify heat transfer. Seismic imaging will be vital for resolving structural and permeability controls, refining thermal regimes, and identifying viable targets.

Future work should emphasise quantitative uncertainty and sensitivity analysis, integration of 3D crustal and permeability models, and coupled thermo-hydraulic simulations to assess depletion and recharge dynamics. Expanded offshore heat-flow and borehole datasets are essential for empirical calibration and validation of global models. Given that cascading-use offshore geothermal architectures remain largely conceptual, future thermo-hydraulic and techno-economic models must be capable of representing these emerging system designs, assessing how resource behaviour and thermal recharge dynamics would affect their operational feasibility and economic viability.

5 CONCLUSIONS

This study presents the first global, physics-based quantification of recoverable offshore geothermal energy. Unlike earlier conceptual assessments, the results derive directly from fundamental heat-transfer equations constrained by globally consistent geophysical datasets, providing a reproducible and scalable estimate of the thermal energy accessible beneath the oceans.

Together, the Viridien white paper (Bolton et al., 2024) and the present analysis establish both the strategic vision and the quantitative foundation for offshore geothermal development. The model yields the first global, data-constrained estimate of recoverable offshore geothermal power, indicating a theoretical capacity of ~6 TWe. These results reinforce the premise that offshore geothermal is a green-energy resource of global significance, while also demonstrating that its magnitude and distribution could support a new generation of integrated offshore-energy systems. As illustrated in Figure 1, such systems could combine firm power generation with CO_2 storage and the co-production of hydrogen, ammonia, and mineral-rich brines.

The spatial variability mapped in this study suggests that these cascading-use configurations, and their associated value propositions, will differ between geological settings. This highlights both the frontier nature of these concepts and the need for location-specific techno-economic models capable of assessing multiple development pathways rather than assuming uniform, electricity-only deployment. In this context, the present analysis provides the quantitative resource framework required to identify where integrated offshore geothermal systems are most likely to prove technically feasible and economically competitive.

REFERENCES

Arnórsson, S.: Major element chemistry of the geothermal sea water at Reykjanes and Svartsengi, Iceland, Geochimica et Cosmochimica Acta, **42**, (1978), 33–44.

Bolton, R., Crossley, R., Fowler, A., Schwarz-Schampera, U. and Njue, L.: Offshore geothermal: A Green energy Resource of Global Significance and its Responsible Development , CGG (now Viridien)/ISA white paper,(2024)

Boyer, T.P., Antonov, J.I., Garcia, H.E., Johnson, D.R., Locarnini, R.A., Mishonov, A.V., Pitcher, M.T., Baranova, O.K. and Smolyar, I.V.: World Ocean Atlas: Global ocean temperature data, NOAA Technical Report, 68, (2005), 1–46.

Clauser, C., and Huenges, E.: Thermal conductivity of rocks and minerals, in Rock Physics and Phase Relations: A Handbook of Physical Constants, ed. T. J. Ahrens, American Geophysical Union, Washington, D.C. (1995), 105–126.

Elderfield, H., and Schultz, A.: Hydrothermal processes at mid-ocean ridges, Annual Review of Earth and Planetary Sciences, **24**, (1996), 191–224.

Friðleifsson, G. Ó., Elders, W.A. and Zierenberg, R.A.: The Iceland Deep Drilling Project at Reykjanes: Drilling into a seawater-recharged system, Journal of Volcanology and Geothermal Research, **391**, (2020), 106435.

IEA: World Energy Outlook, International Energy Agency, Paris (2025).

Jones, A., Crossley, R., Bolton, R. and Williams, M.: Offshore geothermal resources: quantifying the global opportunity, GET 2025 – 6th EAGE Global Energy Transition Conference & Exhibition, Rotterdam, The Netherlands, (2025).

Laske, G., Masters, G., Ma, Z., and Pasyanos, M. E.: CRUST1.0: A global crustal model at 1°×1°, Geophysical Research Abstracts, **15**, (2013), EGU2013-2658.

Li, C.-F., Lu, Y. and Wang, J.: A global reference model of Curie-point depths based on EMAG2. *Sci. Rep.* **7**, 45129; doi: 10.1038/srep45129 (2017).

Straume, E. O., Gaina, C., Medvedev, S., Hochmuth, K., Gohl, K., Whittaker, J. M., et al.: GlobSed: Updated total sediment thickness in the world's oceans. Geochemistry, Geophysics, Geosystems, 20, 1756–1772. ttps://doi. org/10.1029/2018GC008115 (2019).

Uber Technologies: H3 Geospatial Indexing System, Technical Documentation, San Francisco (2025).

Vosteen, H.-D., and Schellschmidt, R.: Influence of temperature on thermal conductivity, thermal capacity and thermal diffusivity for different types of rock, Physics and Chemistry of the Earth, Parts A/B/C, **28** (9–11), (2003), 499–509.